

# A Novel Rotated Constellation-based LLR Detector for Flexible NOMA based OFDM-IM Scheme

Subham Sabud, *Graduate Student Member, IEEE*, and Preetam Kumar, *Senior Member, IEEE*

**Abstract**—OFDM-IM NOMA is a newly created flexible scheme for future generation communication systems. For the downlink OFDM-IM NOMA system, a low-complexity “rotated constellation based log likelihood ratio (LLR) detector” has been proposed in this work. This detector is able to significantly reduce the complexity by employing the rotating constellation-based concept and the log-likelihood ratio-based algorithm together. Complexity analysis and simulation results show that the proposed detector achieves significantly lower computational complexity and much better error performance than the earlier introduced detectors under different scenarios for the OFDM-IM NOMA scheme.

**Index Terms**—Maximum Likelihood (ML) detector, Log Likelihood Ratio (LLR) detector, OFDM, NOMA, Index Modulation (IM).

## I. INTRODUCTION

Non-orthogonal multiple access (NOMA) has established itself as a potential candidate for addressing the high connectivity density environment and massive data load in 5G, 6G, and beyond wireless communication networks. In power-domain NOMA [1], the same time and frequency resources are shared by several users, who are separated by various power levels according to their channel condition. NOMA can provide high spectral efficiency, low latency, massive connectivity and fairness.

On the other hand, orthogonal frequency division multiplexing (OFDM) is a popular multicarrier transmission technique that has the ability to successfully counter the inter-symbol interference (ISI) brought on by a frequency-selective channel. Using the spatial modulation (SM) concept on OFDM, different techniques have been proposed in [2]–[4]. Among them, index modulated OFDM (OFDM-IM) [4] has proven to be the most promising one. The M-ary signal constellation, as well as the subcarrier indices, carry information in OFDM-IM, Unlike the classical OFDM. As a result, OFDM-IM has better spectral efficiency, error performance, and energy efficiency than the traditional OFDM. Using the IM and SM paradigm in conjunction with cooperative NOMA, several excellent studies have been published. An OFDM-IM system built on co-operative NOMA (C-NOMA) is suggested in [5] and is known as CIM-NOMA. The CDM-NOMA technique, which is basically a co-operative NOMA based dual mode OFDM-IM scheme with superior error performance than the generalised CIM-NOMA (GCIM-NOMA), is introduced in [6]. [7] illustrates the use

of a novel technology named C-NOMA-GQSM in multi-vehicle networks. A new energy-efficient, spectrally-efficient, and flexible transmission method called OFDM-IM NOMA [8] has recently been proposed by merging the OFDM-IM and NOMA techniques, where OFDM-IM provides flexibility with a tunable subcarrier activation ratio and NOMA provides flexibility with a tunable power allocation coefficient. [9] discusses a rather similar technique called IM-NOMA, which differs from the previously proposed NOMA-MCIK [10] and Hybrid IM-NOMA [11] schemes. In conventional NOMA-OFDM, all the available subcarriers are in use for both the users, whereas, in the OFDM-IM NOMA, we have the flexibility of activating the subcarriers partially based on the user’s needs. In spite of having all the benefits listed above, the OFDM-IM NOMA [8] system’s ML-based detection approach suffers from very high computational complexity. In [12], a low-complexity LLR-based detection algorithm is suggested, which is applicable to a more generalized IM-MA scheme. However, in [13] the IM-NOMA [9] system uses a constellation rotation-based low-complexity SIC detection technique and recently for the OFDM-IM NOMA [8] system, a low complexity two-stage LLR detector has been introduced in [14].

In this letter, a novel “rotated constellation based LLR detector” is proposed to address the issue of high detection complexity in the downlink OFDM-IM based flexible NOMA scheme. This proposed detector substantially reduces the complexity by combining the constellation rotation-based concept and the log-likelihood ratio-based algorithm together. Additionally, this detector provides an improved error performance. In this system model, User A’s and User B’s symbols are taken from a  $\pi/2$ -rotated and a 0-rotated constellation, respectively. Therefore, there will not be any interference between user A’s and user B’s transmitted signals. As a result, both user A and user B can directly decode their own signals from the superimposed signal without performing the successive interference cancellation (SIC) process. On the other hand, at the receiver side, the purpose of determining the first stage log-likelihood ratio is to identify the active indices, while the purpose of the second stage log-likelihood ratio is to decode the symbols corresponding to the identified active indices.

## II. OFDM-IM NOMA WITH ROTATED CONSTELLATION BASED ML DETECTOR

This section explains the transceiver architecture of downlink OFDM-IM NOMA employing the rotated constellation based ML detector. A total of  $m_\beta$  information bits pass through the transmitter for user  $\beta$ . Here  $\beta \in \{A, B\}$ , where user A is the near user and user B is the far user.

This work is funded by the Ministry of Electronics and Information technology (MeitY), Government of India, Project no: 0429. (*Corresponding author: Subham Sabud*)

The authors are with the Department of Electrical Engineering, Indian Institute of Technology Patna, Bihar, India-801106 (emails: subham\_2011ee15@iitp.ac.in, pkumar@iitp.ac.in).

$m_\beta$  bits are split into  $G_\beta$  groups, each of which carries  $p_\beta$  bits, so  $p_\beta = m_\beta/G_\beta$ . In order to build an active indices set  $I_\beta(g) = \{i_{\beta,1}(g), \dots, i_{\beta,k_\beta}(g)\}$  for the  $g^{\text{th}}$  subblock and user  $\beta$ , the first  $p_{\beta,1}$  bits among the  $p_\beta$  bits utilize a look-up table approach [4] to choose the  $k_\beta$  active indices from the  $n_\beta$  available indices. The remaining  $p_{\beta,2}$  bits are mapped to the  $k_\beta$  active indices' corresponding  $M_\beta$ -ary modulated symbols. Here  $g = 1, \dots, G_\beta$ . In this constellation rotation-based system model, the near user (A) and the far user (B) will take symbols from a  $\pi/2$ -rotated constellation and a 0-rotated constellation, respectively. For  $g^{\text{th}}$  subblock of user A, the vector of modulated symbols is presented as  $\mathbf{s}_A(g) = [S_{A,1}(g), \dots, S_{A,k_A}(g)]$ , where  $S_{A,\tau}(g) \in e^{j\pi/2} Q_{M_A} = Q'_{M_A}$  and  $\tau = 1, \dots, k_A$ . For  $g^{\text{th}}$  subblock of user B, the vector of modulated symbols is presented as  $\mathbf{s}_B(g) = [S_{B,1}(g), \dots, S_{B,k_B}(g)]$ , where  $S_{B,\nu}(g) \in Q_{M_B} = Q'_{M_B}$  and  $\nu = 1, \dots, k_B$ . Here  $Q'_{M_A} = \{q_0^A, \dots, q_{M_A-1}^A\}$  and  $Q'_{M_B} = \{q_0^B, \dots, q_{M_B-1}^B\}$  represent the  $\pi/2$ -rotated constellation corresponding to user A and the 0-rotated constellation corresponding to user B, respectively. Therefore, each subblock fetches a total of  $p_\beta = p_{\beta,1} + p_{\beta,2} = \lfloor \log_2(C(n_\beta, k_\beta)) \rfloor + k_\beta \log_2(M_\beta)$  bits of information. The main OFDM-IM block for user  $\beta$  is produced as  $\mathbf{x}_\beta = [x_\beta(1) \dots x_\beta(N)]^T \in \mathbb{C}^{N \times 1}$ , taking into account  $I_\beta(g)$  and  $\mathbf{s}_\beta(g)$  for all the subblocks. Here  $N = n_\beta G_\beta$  represents the overall number of subcarriers. The superimposed signal in the frequency domain is obtained as  $\mathbf{x}_{sc} = \sqrt{\gamma P_T} \mathbf{x}_A + \sqrt{(1-\gamma)P_T} \mathbf{x}_B$ , where  $\gamma$  and  $P_T$  are the power allocation factor and the total transmit power per subcarrier, respectively. Per subcarrier, the average power assigned to user A and user B is  $P_A = \gamma P_T$  and  $P_B = (1-\gamma)P_T$ , respectively. After applying the inverse fast fourier transform (IFFT) and cyclic prefix addition (CP) operation on  $\mathbf{x}_{sc}$ , the resultant signal is transmitted through a frequency-selective Rayleigh fading channel. The time domain portrayal of the channel impulse response coefficient vector for user  $\beta$  is  $\mathbf{h}_{T,\beta} = [h_{T,\beta}(1) \dots h_{T,\beta}(L)]^T$ , where  $h_{T,\beta}(\rho), \rho = 1 \dots L$  are circularly symmetric and obey  $\mathcal{CN}(0, \frac{1}{L})$  distribution.

Following the CP removal and fast fourier transform (FFT) operations at the receiver side, the signal received for user  $\beta$  in the frequency domain can be represented as  $\mathbf{y}_\beta = \mathbf{x}_{sc} \text{diag}(\mathbf{h}_{F,\beta}) + \mathbf{w}_\beta = [y_\beta(1) \dots y_\beta(N)]^T$ . Here,  $\mathbf{h}_{F,\beta} = \text{FFT}\{\mathbf{h}_{T,\beta}\} = [h_{F,\beta}(1) \dots h_{F,\beta}(N)]^T$  is the channel vector in the frequency domain following  $\mathcal{CN}(0, \varrho_\beta^2)$  distribution and  $\mathbf{w}_\beta = [w_\beta(1) \dots w_\beta(N)]^T$  is the noise vector that obeys  $\mathcal{CN}(0, \sigma_{N_F}^2)$  distribution. Here  $\varrho_\beta^2$  represents the channel gain for user  $\beta$ , and due to the distance factor it is assumed that  $\varrho_A^2 \geq \varrho_B^2$ . As a result,  $P_B > P_A$ . Due to the constellation rotation based system model, the transmitted signal of user A and user B will not interfere with each other. Therefore, both user A and user B can directly decode their own signal from the superimposed signal.  $E_\beta = \{e_{\beta,1}, e_{\beta,2}, \dots, e_{\beta,2^{p_\beta}}\}$  represents the set containing all feasible subblock realizations for performing the rotated constellation based ML detection for user  $\beta$ .

The  $g^{\text{th}}$  subblock of the user  $\beta$ 's signal is directly decoded

using the ‘‘rotated constellation based ML detector’’ as follows.

$$\hat{\mathbf{x}}_\beta^g = \arg \min_{\mathbf{e}_\beta \in E_\beta} \left\| \mathbf{y}_\beta^g - \sqrt{P_\beta} \text{diag}(\mathbf{h}_{F,\beta}^g) \mathbf{e}_\beta \right\|^2, \quad (1)$$

where  $\mathbf{h}_{F,\beta}^g = [h_{F,\beta}(n_\beta(g-1)+1) \dots h_{F,\beta}(n_\beta g)]^T \in \mathbb{C}^{n_\beta \times 1}$ , and  $\mathbf{y}_\beta^g = [y_\beta(n_\beta(g-1)+1) \dots y_\beta(n_\beta g)]^T \in \mathbb{C}^{n_\beta \times 1}$  are the channel vector and the received signal vector for the  $g^{\text{th}}$  subblock of user  $\beta$ , respectively. Here  $\beta \in \{A, B\}$ .

### III. PROPOSED DETECTOR

In this section, the proposed ‘‘rotated constellation-based LLR detector’’ has been discussed.

In this system model, the symbols of user A and user B are taken from a  $\pi/2$ -rotated and a 0-rotated constellation, respectively. Therefore, user A's and user B's transmitted signals will not interfere with each other. As a result, both user A and user B can decode directly their signals from the superimposed signal. For direct decoding of user  $\beta$ 's signal, the ‘‘constellation rotation-based LLR detector’’ is employed as follows.

1) *First stage*: Identifying the active subcarrier indices is the receiver's first stage objective. To accomplish this, it first calculates a log-likelihood ratio for each subcarrier index, taking into account that the symbols in the frequency domain can have either non-zero or zero values. For index  $\delta$ , the first stage log-likelihood ratio can be expressed as follows:

$$\lambda_{\text{stage1},\beta}(\delta) = \ln \frac{\sum_{\mu=0}^{M_\beta-1} P(x_\beta(\delta) = q_\mu^\beta | y_\beta(\delta))}{P(x_\beta(\delta) = 0 | y_\beta(\delta))}. \quad (2)$$

Further (2) can be written [4] as follows by applying the Bayes' formula:

$$\begin{aligned} \lambda_{\text{stage1},\beta}(\delta) &= \ln(k_\beta) - \ln(n_\beta - k_\beta) + \frac{|y_\beta(\delta)|^2}{\sigma_{N_F}^2} \\ &+ \ln \left( \sum_{\mu=0}^{M_\beta-1} \exp \left( \frac{-|y_\beta(\delta) - \sqrt{P_\beta} h_{F,\beta}(\delta) q_\mu^\beta|^2}{\sigma_{N_F}^2} \right) \right), \quad (3) \end{aligned}$$

where  $q_\mu^\beta \in Q'_{M_\beta}$  and  $\delta = 1, \dots, N$ . Here  $\beta \in \{A, B\}$ .

(3) can be simplified [4] as follows for the BPSK modulation:

$$\begin{aligned} \lambda_{\text{stage1},\beta}(\delta) &= \max(c_\beta, d_\beta) + \frac{|y_\beta(\delta)|^2}{\sigma_{N_F}^2} \\ &+ \ln(1 + \exp(-|d_\beta - c_\beta|)), \quad (4) \end{aligned}$$

where  $c_\beta = -|y_\beta(\delta) - \sqrt{P_\beta} h_{F,\beta}(\delta) q_1^\beta|^2 / \sigma_{N_F}^2$  and  $d_\beta = -|y_\beta(\delta) - \sqrt{P_\beta} h_{F,\beta}(\delta) q_0^\beta|^2 / \sigma_{N_F}^2$ . From (4),  $N$  number of LLR values are determined. Then, for each subblock  $g$ , we compute a total  $R_\beta$  number of LLR sums for the  $R_\beta$  sets of feasible active indices combinations provided by the associated look-up table, where  $R_\beta = 2^{p_{\beta,1}}$ . The set containing all feasible active indices combinations for the  $g$  th subblock is indicated as  $\psi_{g,\beta} = \{I_{g,\beta}^1, \dots, I_{g,\beta}^{R_\beta}\}$ , where  $I_{g,\beta}^\nu = \{i_{g,\beta,1}^\nu, \dots, i_{g,\beta,k_\beta}^\nu\}$  for  $\nu = 1, \dots, R_\beta$ . The expression

$J_{g,\beta}^\nu = \sum_{\zeta=1}^{k_\beta} \lambda_{stage1,\beta} \left( n_\beta(g-1) + i_{g,\beta,\zeta}^\nu \right)$  computes the LLR sums that correspond to the  $\nu$  th active subcarrier indices set, where  $g = 1, \dots, G_\beta$  and  $\nu = 1, \dots, R_\beta$ . Thus, for each subblock  $g$ , a total  $R_\beta$  number of LLR sums are obtained. The receiver selects the active indices set with the highest LLR sum among them. That is  $\hat{\nu}_g = \arg \max_{\nu} J_{g,\beta}^\nu$  and the detected active indices set is  $I_{g,\beta}^{\hat{\nu}_g}$ .

2) *Second stage*: Finding constellation symbols corresponding to the detected active subcarrier indices set is the receiver's second stage objective. In order to do that, it calculates a log-likelihood ratio for each subcarrier index, taking into account that the frequency domain symbols can have a value of either  $q_0^\beta$  or  $q_1^\beta$ , under the assumption that the modulation type is BPSK modulation. for index  $\delta$ , it is possible to compute this second stage log-likelihood ratio as follows.

$$\lambda_{stage2,\beta}(\delta) = \ln \frac{P(x_\beta(\delta) = q_0^\beta | y_\beta(\delta))}{P(x_\beta(\delta) = q_1^\beta | y_\beta(\delta))}. \quad (5)$$

Applying Bayes' formula, (5) is expressed as:

$$\lambda_{stage2,\beta}(\delta) = d_\beta - c_\beta, \quad \delta = 1, \dots, N. \quad (6)$$

The second stage receives knowledge from the first stage regarding the detected active indices set. This set's denotation for the  $g$  th subblock is  $I_{g,\beta}^{\hat{\nu}_g} = \{i_{g,\beta,1}^{\hat{\nu}_g}, \dots, i_{g,\beta,k_\beta}^{\hat{\nu}_g}\}$ , where  $i_{g,\beta,\zeta}^{\hat{\nu}_g} \in \{1, \dots, n_\beta\}$  for  $\zeta = 1, \dots, k_\beta$ , here  $\hat{\nu}_g \in \{1, \dots, R_\beta\}$  for  $g = 1, \dots, G_\beta$ . The following is the algorithm of the second stage symbol decoding:

---

**Algorithm 1** Second stage decoding algorithm

---

```

1: for  $\beta = A, B$  do
2:   for  $g = 1$  to  $G_\beta$  do
3:     for  $\zeta = 1$  to  $k_\beta$  do
4:       if  $\lambda_{stage2,\beta}^g(i_{g,\beta,\zeta}^{\hat{\nu}_g}) \geq 0$  then
5:         decoded symbol is  $q_0^\beta$  i.e.  $\vec{x}_\beta^g(i_{g,\beta,\zeta}^{\hat{\nu}_g}) = q_0^\beta$ ;
6:       else if  $\lambda_{stage2,\beta}^g(i_{g,\beta,\zeta}^{\hat{\nu}_g}) < 0$  then
7:         decoded symbol is  $q_1^\beta$  i.e.  $\vec{x}_\beta^g(i_{g,\beta,\zeta}^{\hat{\nu}_g}) = q_1^\beta$ ;
8:       end if
9:     end for
10:   end for
11: end for

```

---

Here  $\lambda_{stage2,\beta}^g(i_{g,\beta,\zeta}^{\hat{\nu}_g}) = \lambda_{stage2,\beta} \left( n_\beta(g-1) + i_{g,\beta,\zeta}^{\hat{\nu}_g} \right)$ . Following the preceding steps, the decoded  $g$  th subblock of user  $\beta$ 's signal is formed as  $\vec{x}_\beta^g = \left[ \vec{x}_\beta^g(1) \dots \vec{x}_\beta^g(n_\beta) \right]^T$ , where  $\vec{x}_\beta^g(\varphi) \in \{0, q_0^\beta, q_1^\beta\}$  for  $\varphi = 1, \dots, n_\beta$ .

#### IV. PERFORMANCE ANALYSIS

In this section, the computational complexity of the proposed detector is investigated at both user A and user B, and it is compared with the existing detectors in the literature.

Computational complexity is quantified via the number of complex multiplications.

At user B, the computational complexity of the ‘‘ML detector’’ derived from [8, eq.(6)] is  $\sim \mathcal{O}(k_B R_B (M_B)^{k_B})$  per subblock, and the computational complexity of the ‘‘rotated constellation based ML detector’’ derived from (1) is  $\sim \mathcal{O}(k_B R_B (M_B)^{k_B})$  per subblock. That is, the ‘‘ML detector’’ and the ‘‘rotated constellation based ML detector’’ have the same computational complexity at user B. On the other hand, The computational complexity of the ‘‘two-stage LLR detector’’ obtained from [14, eq.(5)] is  $\sim \mathcal{O}(n_B M_B)$  per subblock, and the computational complexity of the ‘‘proposed detector’’ obtained from (3) is  $\sim \mathcal{O}(n_B M_B)$  per subblock. In other words, the computational complexity of the ‘‘two-stage LLR detector’’ and the ‘‘proposed detector’’ comes out to be the same at user B. Note that, for user B,  $\beta = B$  in (1) and (3).

At user A, the total computational complexity of the ‘‘ML detector’’ computed from [8, eq.(3)] and [8, eq.(5)] is  $\sim \mathcal{O}(k_B R_B (M_B)^{k_B} + k_A R_A (M_A)^{k_A})$  per subblock. While the computational complexity of the ‘‘rotated constellation-based ML detector’’ calculated from (1) is  $\sim \mathcal{O}(k_A R_A (M_A)^{k_A})$  per subblock. On the other hand, at user A, the total computational complexity of the ‘‘two-stage LLR detector’’ determined from [14, eq.(10)] and [14, eq.(15)] is  $\sim \mathcal{O}(n_B M_B + n_A M_A)$  per subblock. while the computational complexity of the ‘‘proposed detector’’ derived from (3) is  $\sim \mathcal{O}(n_A M_A)$  per subblock. Note that, for user A,  $\beta = A$  in (1) and (3).

From the above analysis, it can be seen that the proposed detector has significantly less computational complexity than the conventional ML detector. At user B, the reason for the much reduced complexity of the proposed detector is the log-likelihood ratio (LLR) based algorithm used in it. While at user A, there are two reasons for the complexity reduction of the proposed detector. First, due to the use of the LLR-based algorithm. Second, due to the use of the rotated constellation-based concept, the receiver can directly decode user A's signal without needing to go through the SIC process at user A. For better understanding, the following TABLE I, TABLE II, and TABLE III show the complexity reduction of different detectors as compared to the conventional ML detector in various scenarios.

TABLE I: Complexity reduction as compared to the optimal ML detector where both the users having mid data rate application (i.e.  $k_A = k_B = 2$ ,  $n_A = n_B = n = 4$ ,  $M_A = M_B = M = 2$ ).

Detector type	Complexity reduction at user B	Complexity reduction at user A
Rotated ML	0%	50%
Two-stage LLR	75%	75%
Proposed	75%	87.5%

#### V. SIMULATION RESULTS

This section presents the simulation results of the error performance of the proposed detector in presence of the Rayleigh fading channel and compares it with the error performance of

TABLE II: Complexity reduction as compared to the optimal ML detector where both the users having high data rate application (i.e.  $k_A = k_B = 3$ ,  $n_A = n_B = n = 4$ ,  $M_A = M_B = M = 2$ ).

Detector type	Complexity reduction at user B	Complexity reduction at user A
Rotated ML	0%	50%
Two-stage LLR	91.7%	91.7%
Proposed	91.7%	95.8%

TABLE III: Complexity reduction as compared to the optimal ML detector for the hybrid user specification (i.e.  $k_A = 3$ ,  $k_B = 1$ ,  $n_A = n_B = n = 4$ ,  $M_A = M_B = M = 2$ ).

Detector type	Complexity reduction at user B	Complexity reduction at user A
Rotated ML	0%	25%
Two-stage LLR	75%	87.5%
Proposed	75%	93.75%

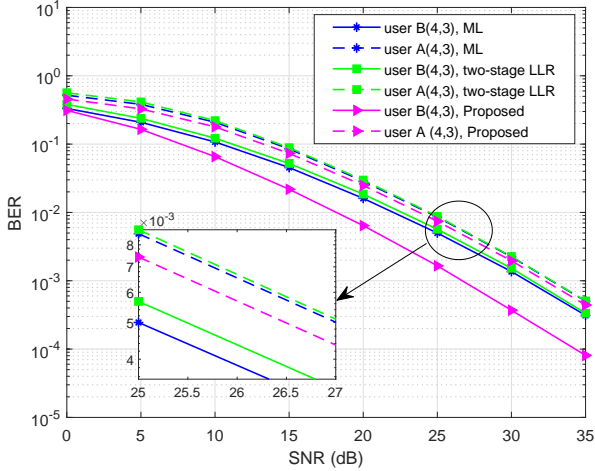


Fig. 1: Comparing BER of the proposed detector with the “ML detector” and the “two-stage LLR detector”, where both users have high data rate applications

the “ML detector”, the “two-stage LLR detector” [14] and the “rotated constellation based ML detector”. The system parameters used for all the simulations are:  $N = 256$ ,  $G_A = G_B = 64$ ,  $n_A = n_B = n = 4$ ,  $\rho_A^2 = 4$  dB,  $\rho_B^2 = 0$  dB,  $N_{cp} = 16$ ,  $L = 12$ ,  $\gamma = 0.1$ , and  $M_A = M_B = M = 2$ .

With a same-user application taken into account, Fig. 1 compares the BER performance of the proposed detector with the BER performance of the “ML detector” and the “two-stage LLR detector”. By setting the simulation parameter to  $k_A = k_B = 3$ ,  $n = 4$ , it is assumed that both users having high data rate applications (e.g. ultrahigh definition video streaming) utilize the same NOMA spectrum. Therefore, an identical subcarrier activation ratio of  $3/4$  is considered for both users in this case. From this figure, we can observe that at user B, the proposed detector achieves a gain of 4 dB at a BER of  $10^{-3}$ , when compared to the “ML detector” and the “two-stage LLR detector”. While, at user A, the proposed detector attains a slightly better error performance than the optimal ML detector and the two-stage LLR detector at a BER of  $10^{-3}$ .

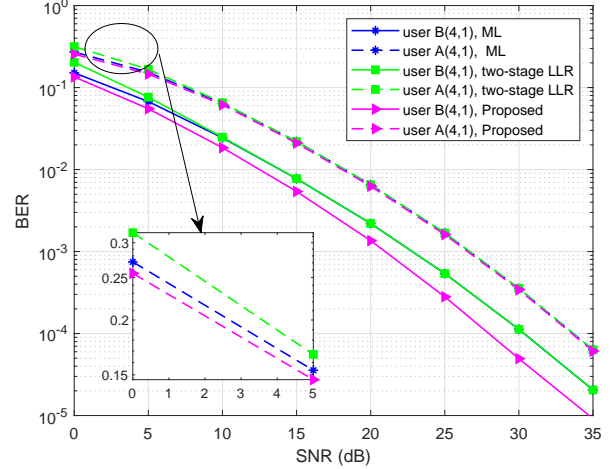


Fig. 2: Comparing BER of the proposed detector with the “ML detector” and the “two-stage LLR detector”, where both users have low data rate applications

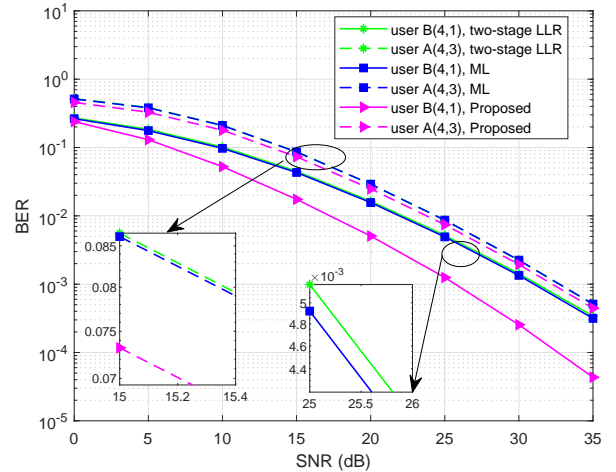


Fig. 3: Comparing BER of the proposed detector with the “ML detector” and the “two-stage LLR detector” for the hybrid user configuration

Considering another same-user application, Fig. 2 compares the BER performance of the proposed detector with the BER performance of the “ML detector” and the “two-stage LLR detector”. By setting the simulation parameter to  $k_A = k_B = 1$ ,  $n = 4$ , it is assumed that both users having low data rate applications (e.g. Internet of Things application) are utilizing the same NOMA spectrum. Therefore, an identical subcarrier activation ratio of  $1/4$  is considered for both users in this case. According to this figure, at user B, the proposed detector achieves a gain of 2 dB at a BER of  $10^{-3}$ , when compared to the “ML detector” and the “two-stage LLR detector”. While at user A, the proposed detector achieves a minute improvement in error performance over the ML detector and the two-stage LLR detector at a BER of  $10^{-3}$ .

For a hybrid-user application, Fig. 3 compares the BER performance of the proposed detector with the BER perfor-

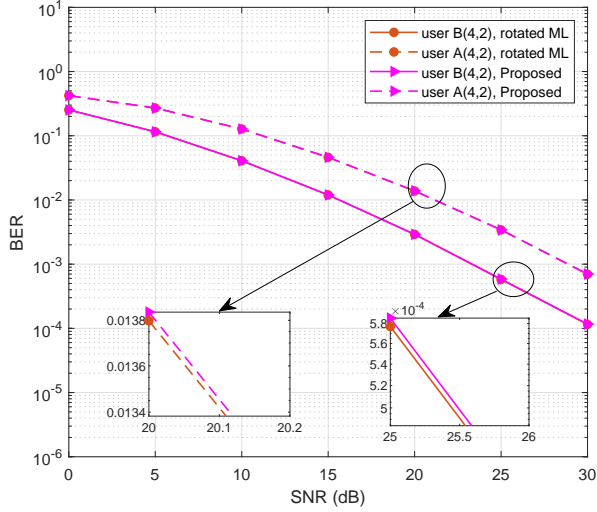


Fig. 4: Comparing BER of the proposed detector with the BER of the “rotated constellation-based ML detector”

mance of the “ML detector” and the “two-stage LLR detector”. Since user A and user B with different settings are utilizing the same spectrum, the users in this scenario are referred to as hybrid users. By setting the simulation parameter to  $k_A = 3, k_B = 1, n = 4$ , it is considered that the user A with a high data rate application and user B with a low data rate application utilize the same NOMA spectrum. Therefore, a subcarrier activation ratio of 3/4 and 1/4 is assigned to user A and user B, respectively. Fig. 3 shows that at user B, the proposed detector achieves a gain of 5.5 dB at a BER of  $10^{-3}$  when compared to the “ML detector” and the “two-stage LLR detector”. While, at user A, the proposed detector achieves a slightly better error performance than the optimal ML detector and the two-stage LLR detector at a BER of  $10^{-3}$ .

In Fig. 4, the error performance of the proposed detector is compared with that of the “rotated constellation-based ML detector”. This figure illustrates that the proposed detector obtains nearly identical error performance as the “rotated constellation-based ML detector”, while the proposed detector has much reduced computational complexity than the “rotated constellation-based ML detector” at both user A and user B, as indicated in the previous performance analysis section.

## VI. CONCLUSION

In this paper, a novel “constellation rotation-based LLR detector” is proposed for the OFDM-IM NOMA scheme. This proposed detector is evaluated under several scenarios, including users with high data rate applications, low data rate applications, and hybrid applications. Simulation results and complexity analysis demonstrate that in every case, the proposed detector achieves significantly lower computational complexity while also achieving much better error performance than the earlier introduced detectors in the literature.

## REFERENCES

[1] Y. Liu *et al.*, “Nonorthogonal Multiple Access for 5G and Beyond,” *Proc. IEEE*, vol. 105, no. 12, pp. 2347–2381, Dec. 2017.

[2] R. Abu-alhiga and H. Haas, “Subcarrier-index modulation OFDM,” in *2009 IEEE 20th International Symposium on Personal, Indoor and Mobile Radio Communications*, 2009, pp. 177–181.

[3] D. Tsonev, S. Sinanovic, and H. Haas, “Enhanced subcarrier index modulation (SIM) OFDM,” in *2011 IEEE GLOBECOM Workshops (GC Wkshps)*, 2011, pp. 728–732.

[4] E. Başar, U. Aygözü, E. Panayırıcı, and H. V. Poor, “Orthogonal Frequency Division Multiplexing With Index Modulation,” *IEEE Trans. Signal Process.*, vol. 61, no. 22, pp. 5536–5549, Nov. 2013.

[5] X. Chen, M. Wen, and S. Dang, “On the Performance of Cooperative OFDM-NOMA System With Index Modulation,” *IEEE Wireless Commun. Lett.*, vol. 9, no. 9, pp. 1346–1350, Sept. 2020.

[6] X. Chen *et al.*, “Spectrum Resource Allocation Based on Cooperative NOMA With Index Modulation,” *IEEE Trans. Cogn. Commun. Netw.*, vol. 6, no. 3, pp. 946–958, Sept. 2020.

[7] J. Li *et al.*, “Generalized Quadrature Spatial Modulation and its Application to Vehicular Networks With NOMA,” *IEEE Trans. Intell. Transp. Syst.*, vol. 22, no. 7, pp. 4030–4039, July 2021.

[8] E. Arslan, A. T. Dogukan, and E. Basar, “Index Modulation-Based Flexible Non-Orthogonal Multiple Access,” *IEEE Wireless Commun. Lett.*, vol. 9, no. 11, pp. 1942–1946, Nov. 2020.

[9] A. Almohamad, M. O. Hasna, S. Althunibat, and K. Qaraqe, “A Novel Downlink IM-NOMA Scheme,” *IEEE Open j. Commun. Soc.*, vol. 2, pp. 235–244, Feb. 2021.

[10] E. Chatziantoniou, Y. Ko, and J. Choi, “Non-Orthogonal Multiple Access with Multi-carrier Index Keying,” in *European Wireless 2017; 23th European Wireless Conference*, 2017, pp. 1–5.

[11] A. Tusha, S. Doğan, and H. Arslan, “A Hybrid Downlink NOMA With OFDM and OFDM-IM for Beyond 5G Wireless Networks,” *IEEE Signal Process. Lett.*, vol. 27, pp. 491–495, Mar. 2020.

[12] J. Li, Q. Li, S. Dang, M. Wen, X.-Q. Jiang, and Y. Peng, “Low-Complexity Detection for Index Modulation Multiple Access,” *IEEE Wireless Commun. Lett.*, vol. 9, no. 7, pp. 943–947, Feb. 2020.

[13] A. Almohamad *et al.*, “Low Complexity Constellation Rotation-based SIC Detection for IM-NOMA Schemes,” in *2020 IEEE 92nd Veh. Technol. Conf. (VTC2020-Fall)*, 2020, pp. 1–5.

[14] S. Sabud and P. Kumar, “A Low Complexity Two-stage LLR Detector for Downlink OFDM-IM NOMA,” *IEEE Commun. Lett.*, pp. 1–1, 2022.